Fall Detection using Wi-Fi Signals and Threshold-Based Activity Segmentation

Robert M. Keenan and Le-Nam Tran
School of Electrical and Electronic Engineering
University College Dublin
Dublin, Ireland
Email: robert.keenan.2@ucdconnect.ie, nam.tran@ucd.ie

***Abstract*—We present the design and implementation of a low-cost, accurate and non-invasive wireless fall detection system utilising commercial off-the-shelf (COTS) 802.11n WLAN network interface cards (NICs). The system utilises the channel state information (CSI) of the wireless channel between a transmitter and a receiver. Notably, in addition to the CSI amplitude, the proposed system exploits the phase difference over 2 receiving antennas to detect patterns uniquely attributed to a human falling. Our extensive experimental results show that the CSI phase difference is a more granular measure at $5\,\text{GHz}$ rather than the amplitude. The proposed method for fall detection consists of two stages. In the first stage, we quickly segment two types of actions, fall-like activities and falling activities to reduce the computational power required. In the second stage, we build a classification algorithm with newly defined features to detect three types of falls, namely walking-falls, standing-falls and sitting-falls. The concept of a sitting-fall is introduced whereby a person falls as they are standing up or sitting down. This is much more subtle than a walking-fall or standing-fall. To this end we introduce new features for signal classification such as the velocity of change of the standard deviation of the CSI phase difference. We also improve on existing features such as TimeLag proposed in [1]. We carry out extensive experiments to evaluate the performance of the proposed fall detection system. Particularly, the results demonstrate a balanced accuracy of $96\,\%$ for the proposed system, compared to $91\,\%$ for the top state-of-the-art solution [1].**

***Index Terms*—Fall detection, channel state information (CSI), activity classification, Wi-Fi, phase difference**

I. Introduction

Falls are one of the leading causes of fatal and non-fatal injuries especially for elderly people in today's society. Quick response is vital to reducing the long-term effects on the victim physically, emotionally and mentally [2], [3]. Falls, especially among the elderly, place a severe strain on health and financial systems around the world costing the US healthcare system \$50bn in 2015 [4].

Over $50\,\%$ of falls for the 65+ age group (1/3 experience a fall at least once a year) occur in their home so a solution that is **cheap, accurate, privacy-focused** and **easily installed**, is needed [3], [4]. Falls can have great effects on elderly people and the fear induced in a fall victim post-treatment can deem them unable to live independently in the future [5].

There are a number of solutions on the commercial market today which can be divided into a broad number of categories such as wearables, visual devices and ambient environment sensors. Products on the market in these categories include the Apple Watch, cameras, accelerometer belts, floor vibration sensors and infrared devices. Privacy is a key issue nowadays and as such, is a primary aim for our proposed system. Many of the current solutions on the market suffer from privacy issues especially in such a sensitive environment as somebody's home. Many of these off-the-shelf solutions require direct Line of Sight (LOS) to the person in the room to detect a fall. No obstacles can be in the way of the detection apparatus, otherwise a fall may not be detected by the system. This is especially problematic in a busy household environment with many obstacles. All of the existing solutions mentioned above are very expensive to buy and implement such as the Apple Watch, specialist cameras and Man-Down alarms. Another issue arises as elderly people are not inclined to wear them as they hinder them from daily activities. A solution that does not hinder a person's daily way of life is needed, as a requirement to wear a device leads to issues in terms of battery charge, precise locations on the body and the refusal of some people to wear the devices. More complex solutions such as Computer Vision cameras require high processing power for the calculations and classification operations needed for the sheer amount of data recovered in any of these fall detection experiments.

To tackle the above issues, we present a Wi-Fi based fall detection solution using COTS NICs in this paper. In particular, the proposed system provides a cheap, highly accurate and non-intrusive fall detection method for the home and other environments using the Linux CSI tool [6]. Our proposed solution capitalises and improves upon the previous works on this research direction such as [1], [7].

II. Preliminaries

In this section we provide some preliminaries regarding the concept of fall detection using Wi-Fi systems and carry out initial investigations using existing methods in [1], [7]–[10]. The system model of interest consists of a transmitter and a receiver, where the number of antennas at the transmitter and receiver is N_{TX} and N_{RX}, respectively. As an OFDM Wi-Fi system is involved, data transmission occurs in a number of subcarriers. The number of data subcarriers depends on the total system bandwidth of the considered Wi-Fi system. For example, this number is 52 for the $5\,\text{GHz}$ 802.11n standard with a $20\,\text{MHz}$ bandwidth. Let $\mathbf{x}_k \in \mathbb{C}^{N_{TX}\times 1}$ be the transmitted signal over

978-1-7281-4490-0/20/\$31.00 © 2020 IEEE

978-1-7281-4490-0/20/\$31.00 ©2020 IEEE

subcarrier k, where the notation $\mathbb{C}^{m\times n}$ denotes the complex space of size $m \times n$. Then the received signal at subcarrier k is given by

$$\mathbf{y}_k = \mathbf{H}_k\mathbf{x}_k + \mathbf{n}_k \tag{1}$$

where $\mathbf{H}_k \in \mathbb{C}^{N_{TX}\times N_{RX}}$ is the wireless channel between transceivers over subcarrier k, $\mathbf{n}_k$ is the noise vector.

In practice, the channel state information (CSI) for Wi-Fi systems is denoted by $\mathbf{H}$ and normally defined as the 3-D matrix stacking $\mathbf{H}_k$ for all k in a new dimension. The third dimension (i.e. the depth) of the CSI matrix $\mathbf{H}$ is ideally equal to the number of subcarriers. However, depending on a specific NIC device, $\mathbf{H}_k$ is only measured for some subcarriers. For example the Intel Wi-Fi Link 5300 802.11n NIC utilised in this paper only reports the estimate of $\mathbf{H}_k$ for 30 groups out of 52 data subcarriers for a 5 GHz channel.

The channel between the m-th transmit antenna and the n-th receive antenna over subcarrier k is denoted by $h_{k,mn}$. Note that the complex baseband equivalent channel model is used, and thus $h_{k,mn}$ is a complex number which can be expressed as [11]

$$h_{k,mn} = |h_{k,mn}|e^{j\phi_{k,mn}} \tag{2}$$

where $j = \sqrt{-1}$. We refer to $|h_{k,mn}|$ and $\phi_{k,mn}$ as the CSI amplitude and the CSI phase, respectively. Any change in the channel introduced by either path loss or multi-path fading will result in channel distortion (amplitude distortion and phase shift). For a stable channel (no people), each subcarrier will not be distorted by small-scale fading caused by human activities. However, a human introduced to the environment will cause variations to the channel and this will be reflected in the CSI matrix. In our work we build the proposed system on a specific Intel NIC and use the Linux CSI tool [6] to obtain the CSI matrix of size $N_{TX} \times N_{RX} \times 30$ per packet.

A. CSI Amplitude

To the best of our knowledge, RT-Fall [1] and WiFall [7] are currently the state-of-the-art systems in the field of fall detection using Wi-Fi systems. These systems found that the different CSI streams are affected independently by human activities while different subcarriers in those streams are affected in similar ways. A stream is defined as the link between 2 respective antennas. The CSI amplitude returned by the Linux CSI tool tends to be quite noisy and uninformative. Hence, the CSI samples are averaged over 30 subcarrier values to obtain a single representative value for each stream. This allows for simpler computation when operating multiple streams at once. For a given packet, the effective CSI of the stream between transmit antenna m and receive antenna n is calculated by averaging the CSI amplitude of 30 measured subcarrier groups as [8]

$$CSI_{mn} = \frac{1}{N}\sum_{k=1}^{N}\frac{f_k}{f_0}|CSI_{k,mn}|, \tag{3}$$

where $f_0 = 5$ GHz is the centre frequency, f_k is the frequency of subcarrier k around the centre frequency, and $N = 30$ is the number of measured subcarriers. In the above equation, $CSI_{k,mn}$ is an estimate of $h_{k,mn}$ in (2)

B. CSI Phase Difference

For a given subcarrier f, the CSI phase $\hat{\phi}_f$ obtained by the CSI tool [6] contains an unknown phase offset β, time lag Δt and measurement noise Z_f as detailed by [12]:

$$\hat{\phi}_f = \phi_f + 2\pi f_f \Delta t + \beta + Z_f. \tag{4}$$

The phase difference between 2 receive antenna is thus:

$$\Delta\hat{\phi}_f = \Delta\phi_f + 2\pi f_f \epsilon + \Delta\beta + \Delta Z_f, \tag{5}$$

where $\Delta\phi_f$ is the true phase difference, $\epsilon = \Delta t_1 - \Delta t_2$, where Δt_1 and Δt_2 are time lags at each corresponding antenna, and $\Delta\beta$ is the unknown constant phase difference offset. This expression yields extremely noisy data and thus, a linear transform is proposed to remove outliers and offsets as done in PhaseU [10], which is given by

$$\tilde{\phi}_f = \hat{\phi}_f + \frac{\phi_N - \phi_1}{k_N - k_1}k_f - \frac{1}{N}\sum_{n=1}^{N}\phi_n, \tag{6}$$

where k_n represents the coefficient of the n-th subcarrier [13, p.53], $\hat{\phi}_f$ is the measured phase and ϕ_n is the phase of subcarrier n. As seen in RT-Fall [1] and PhaseU [10], the phase difference at high frequencies such as 5 GHz is actually the sum of the variance of the phase on each RX antenna as they are both independent. Thus, the phase difference is written as

$$\sigma^2_{\Delta\tilde{\phi}_f} = \sigma^2_{\Delta\tilde{\phi}_{f,1}} + \sigma^2_{\Delta\tilde{\phi}_{f,2}}. \tag{7}$$

where $\sigma^2_{\Delta\tilde{\phi}_{f,i}}, i = 1, 2$ is the variance of the phase at RX antenna i. We use (7) to compute the CSI phase difference in our implemented system.

C. Human Activities & CSI Amplitude/Phase Difference

To test the viability of using CSI amplitude and phase difference for fall detection, experiments were carried out to judge the relationship between human activities and the CSI amplitude. Activities that were both immobile (lying, sitting, standing) and mobile (walking, standing up, sitting down) were performed. For the immobile activities in a typical living room setting, it was found that the amplitude and phase difference stay relatively stable in a home environment with LOS conditions when a person is sitting (cf. Fig. 1(a)). The introduction of a mobile subject to the environment causes variations to both CSI amplitude and phase difference as shown in Fig. 1(b). In particular, the CSI amplitude fluctuates between 23 dB and 27 dB. The multi-path environment introduced by the moving subject makes it hard to identify patterns.

Other mobile activities were considered such as sitting down (fall-like) in Fig. 2(a) and a walking fall in Fig. 2(b). The variance in the CSI amplitude for these actions fluctuates greatly and occasionally does not present clear starting and finishing times. In Fig. 2(b), the subject begins walking at 5 s, and it is clear that something is happening. At 10 s, the subject falls. This is represented by a large disturbance in the phase difference followed by a sudden and sharp profile decline. This same response can be seen at 10 s for the CSI amplitude. However, this

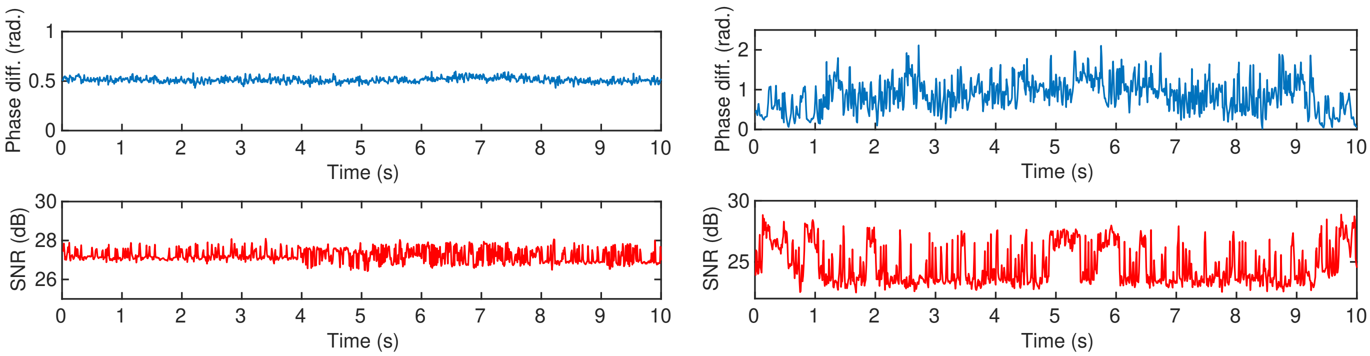

(a) Sitting

(b) Walking

Fig. 1. CSI phase difference (blue) and amplitude (red) of (a) sitting and (b) walking.

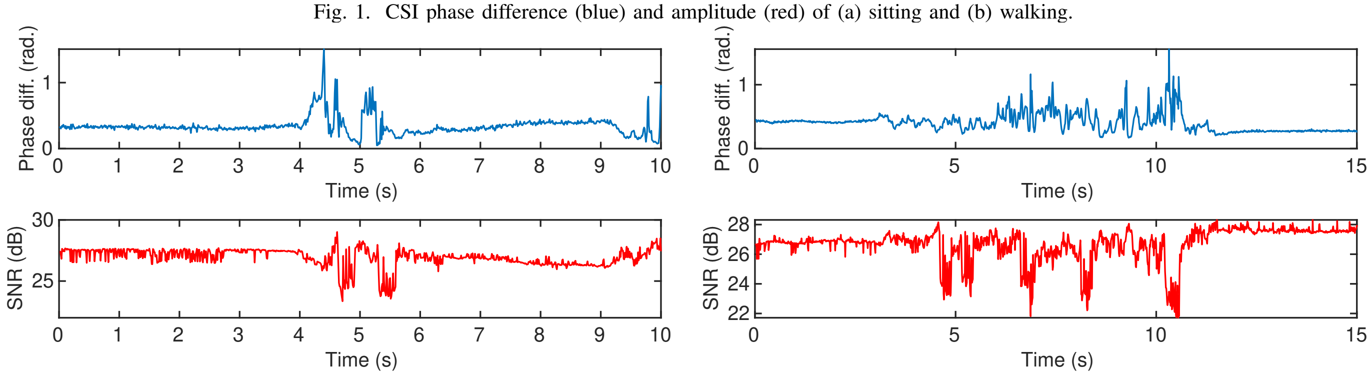

(a) Sitting down

(b) Walking fall

Fig. 2. CSI phase difference (blue) and amplitude (red) of (a) sitting down (fall-like activity) and (b) a walking fall (fall activity).

response is very similar to the response at approx. 5 s, 6 s and 8 s. It is unclear where the activity starts and finishes in comparison to a fall or fall-like activity using the phase difference. The CSI amplitude alone is simply not precise enough for use in activity detection. Our initial investigations also agree with previous studies that, when (6) and (7) are implemented, the system produces a CSI phase difference which is much more granular and identifiable than the amplitude for mobile and immobile activities. Thus, the CSI phase difference at 5 GHz from (7) is utilised for activity finishing point detection/segmentation.

D. *Frequency of Human Activities in different scenarios*

As other fall detection systems have found, the frequency of a human activity can be used to segment different types of activities. The frequency of a human activity is dependent on factors such as the size of the human, the speed at which they are moving and what body parts are moving (limbs vs. their whole body). Unlike WiFall [7], it is proposed to segment activities using their associated frequency. We, similar to RT-Fall [1], propose to remove lower frequency movements such as walking, standing, sitting and retain the higher frequency movements for further analysis. As a result, the computation required for classification can be reduced since it only needs to differentiate between fall and fall-like activities. To this end, we note that fall-like activities such as sitting down, standing up, squatting and jumping have a much higher frequency than immobile activities but do not have the same associated power decline as is common to falling.

A time-frequency analysis of the CSI data was performed to identify fall-like activities from falling activities as shown in Fig. 3 using a Spectrogram (Short Time Fourier Transform). We concur with [1] that fall/fall-like activities occur in the $[5, 10]$ Hz range depending on the size of the person in the environment. The obtained spectrogram in Fig. 3 justifies the use of a filtering technique for higher frequency actions. At 5 s, the subject was walking and the spectrogram shows little to no response. From 15-18 s, the subject sat down. This is demonstrated by a brightening/strong power profile in the spectrogram. At 31 s, the subject stood up from their seat resulting in a power increase shown. From 45-50 s, the subject repeatedly sat down and stood up. Again, this results in a strong power profile. From 55-60 s, the subject jumped continuously but we notice a weaker power profile than sitting down indicating that fall like movements like sitting down are noticeable in the CSI data. At 75 s, the subject fell over after walking for 5 s. This is shown by a bright colour on the spectrogram indicating a very strong power profile with some components reaching 10 Hz due to limb movement.

Hence, it is clear that fall and fall-like movements have strong power profiles with higher frequency components than other movements. A band-pass filter is employed to filter these higher frequencies for analysis.

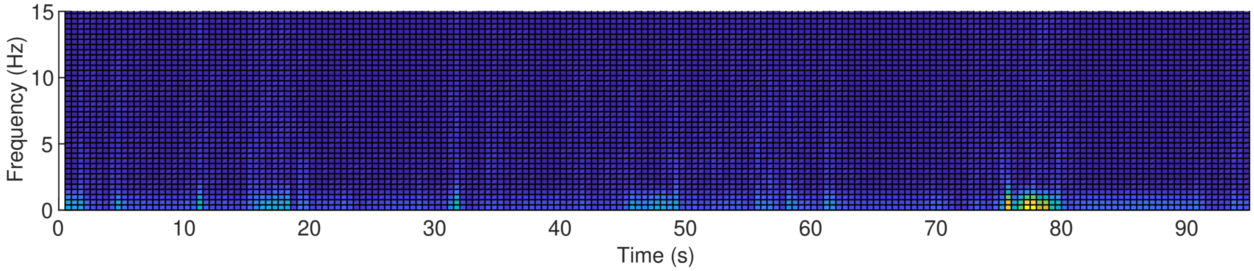

Fig. 3. Spectrogram of a series of Activities of Daily Living (ADL)

III. Proposed Fall Detection System and Signal Classification

The system is divided into a number of subsystems as described below.

A. Signal Pre-processing

1) CSI Cleaning: As mentioned in Section II, the incoming CSI data contains outliers, offsets and noise. These are cleaned from the CSI amplitude and phase difference separately so as to guarantee accurate classification free from noise. For this purpose, we use (3) to obtain a single representative CSI amplitude per stream, rather than using 30 reported CSI values from the CSI tool for each packet. Equation (6) is applied to the CSI phase to remove unwanted phase offsets and noise. Equation (7) is applied to the cleaned CSI phase to compute the CSI phase difference.

2) Interpolation: As noted in (4), there is a time-lag Δt associated with each received packet. A 1-D linear interpolation algorithm is performed using the NIC's internal clock to ensure a TX rate of 100 (pkts/s) and to allow the system to accurately detect activities using the activity segmentation methods.

3) CSI Filtering: A band-pass filter with a pass-band of $[5, 10]$ Hz is implemented as discussed in Section II-D to remove low frequency human activities as in RT-Fall [1]. This reduces the number of activities needing to be segmented for classification utilising less computational power.

B. Activity Segmentation

There are 2 steps to the proposed system's activity segmentation: A threshold based activity finishing time detector and trace back activity segmentation.

1) Identifying the finishing times of activities: At this stage of the process, there are 2 CSI data-sets. One of the band-pass filtered CSI phase difference and another of the non-filtered (i.e. raw) CSI phase difference. The method implemented is similar to that of [1].

A threshold value is established from stationary LOS data of one-minute duration for both the filtered and non-filtered CSI. The threshold value for each data-set is established as $\mu + 6\sigma \leq \delta$, where δ is the threshold value for the individual data-set. Due to the normalisation of the CSI data usually, a threshold value of $\delta = 6\sigma$ is proposed. This threshold is then used to determine if the CSI phase difference has entered a "fluctuating" or "stable" state. To determine the finishing points of activities, a sliding window of 3 seconds (300 packets) slides through both CSI data-sets for a given non-stationary CSI stream, one packet at a time. At each iteration, the standard deviation of the 2 data-sets inside the sliding window is computed. If the standard deviation σ of either CSI stream in the window has fallen below the respective stream's (filtered/non-filtered) threshold value, the signal can be marked as entering a stable state. If it is above the threshold, it is marked as being in a fluctuating state. In RT-Fall, the mean value is used rather than the standard deviation which we propose.

For each sliding window, each signal's state is recorded before a check to see if they occupy the same state. This is used to compute the TimeLag feature which was proposed in [1]. If there is a transition in one of the signals from a fluctuating state to a stable state at t_1, the other signal is tracked to see if the same transition happens within a given time Δt ($t_2 = \Delta t + t_1$). If so, the TimeLag is set as Δt and t_1 is set as the activity's finishing point.

2) Implementing windowing around an activity: A window of size 3 seconds is then applied around these activity finishing points to gather statistical features for classification. This allows the system to capture the entire duration of the fall up until the finishing point (2 seconds) where the majority of the subject's movement takes place and allows 1 second after the fall to determine if the subject is stationary.

C. Feature Extraction

The feature extraction module extracts features from both the CSI amplitude and phase difference in the segmented activity windows. 11 features are gathered: (1) normalised standard deviation, (2) maximum absolute deviation (MAD), (3) offset of the signal strength, (4) interquartile range, (5) mean signal entropy, (6) rate of signal change, (7) TimeLag [1], (8) power decline ratio [1], (9) velocity of signal change, (10) velocity of change of standard deviation and (11) duration under the threshold value. Features 1-6 are calculated using the CSI amplitude and phase difference while features 7-11 are calculated using the CSI phase difference. Features 9-10 are calculated from the start of a window to the falling time. We remark that features 1-8 were proposed in [1], [7], and features 9-11 are newly defined in this paper.

D. Classification

As the CSI filtering stage filters a lot of the stationary and non fall-like activities, the classification problem becomes one of a binary choice: fall or fall-like classification.

To correctly predict a fall, a simple binary classifier is implemented in MATLAB. For training the model, labelled data and features must be provided to the classifier in the form of an *objective* class (falls) and *non-objective* class (fall-like activities).

The data is manually labelled with either a 1 for a fall or -1 for no fall. Once the model is built, test data can be classified by it and any incorrect predictions by the model help to update the model further for extended testing. Two classifiers are implemented in this system, a Support Vector Machine (SVM) and a Bagged Tree Classifier (Ensemble). A bagging ensemble was chosen to reduce variance and an SVM as a comparison to existing systems could be made using this.

IV. Experiments & Results

A. Experimental Setup

The system's experimental setups consisted of one transmitter device, a TP-LINK Archer C6 AP, and one or more receiver devices (laptops) with the appropriate Intel Wi-Fi Link 5300 NIC installed. The laptops had Ubuntu 14.04 LTS installed with customised and modified *iwlwifi* drivers courtesy of the Linux CSI tool [6]. The transmitter and receiver devices were set up in typical residential environments such as a home living room. The packet transmission rate was set at 100 (pkts/s) for the 802.11n network at a centre frequency of 5.2 GHz and a 20 MHz bandwidth. The transmitter and receiver devices were set up a distance of 3.5-5 m from each other at a height of 0.5-1 m from the ground to ensure maximum environment coverage.

Classification training and testing data-sets were gathered by a single subject. Training data consisted of 100 falls gathered over four 20 min experiments. Just over 200 Activities of Daily Living (ADLs) were performed, paying special attention to fall and fall-like activities. These activities were performed continuously to ensure robustness of the model. Four test data-sets of CSI data were gathered in the same indoor home environment with tests of 10-20 min duration with the same subject aiming to ensure a balanced test set between fall and fall-like activities.

B. Performance of Activity Segmentation

To evaluate the proposed activity segmentation system, extended periods of ADLs were performed with a balance of fall and fall-like activities. Five tests of 3-5 min were performed with 10-12 falls performed in each. It was ensured that the activities performed to test the implemented system ranged from faster movements of younger people to slower, more deliberate movements of elderly people. Using a video to verify the tests, the activity segmentation method segments 100 % of performed falls (walking, standing or sitting) as demonstrated by Figs. 4 & 5, proving our method for activity segmentation. Fall-like activities such as standing up, sitting down and dropping objects were detected as expected. It was found that doors opening caused segmentation also. To conclude, the activity segmentation system is consistently accurate while reducing computation in comparison to WiFall [7] with a 100 % segmentation rate.

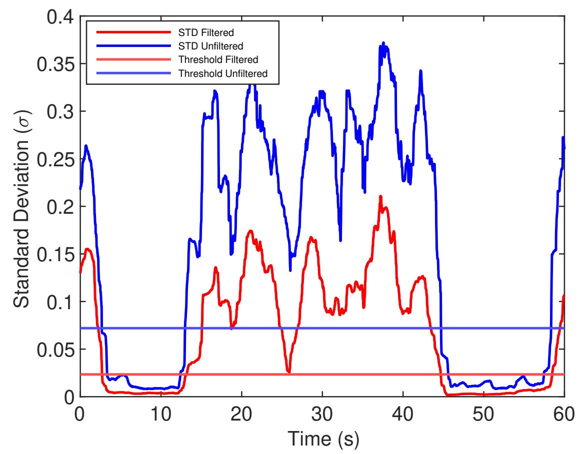

Fig. 4. Threshold-based finishing time detection is demonstrated above. The blue and red horizontal lines represent the unfiltered and filtered CSI phase difference thresholds, respectively. When either trace goes beneath their threshold, a fall or fall-like activity has occurred.

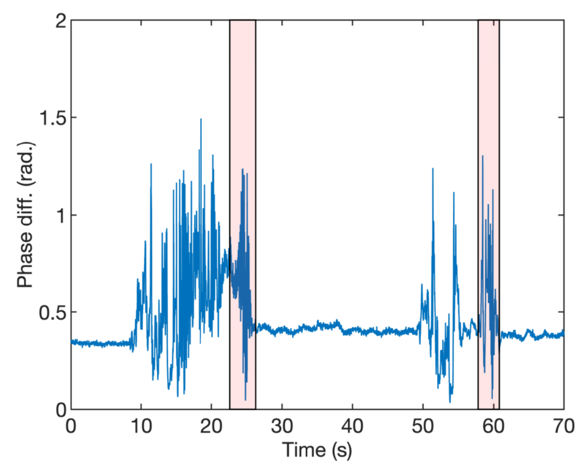

Fig. 5. This demonstrates the activity segmentation around a segmented fall. A window of 3 seconds is obtained (2 s before the fall and 1 s after). Features are then gathered from these windows for classification.

C. Fall Detection Classification

Using the trained classifiers from the features gathered in the Feature Extraction module of the system, the 4 test sets of CSI data and ADLs could be classified. The SVM and Bagged Tree classifier models were used to produce a prediction set which was verified using a video of the test data-set gathering session.

Over the 4 test sets of ADLs performed (50 falls) as mentioned in Section IV-A, Balanced Accuracy, Sensitivity (True Positive Rate), Specificity (True Negative Rate) and F1-Score were used as the measures of classifier performance. Balanced

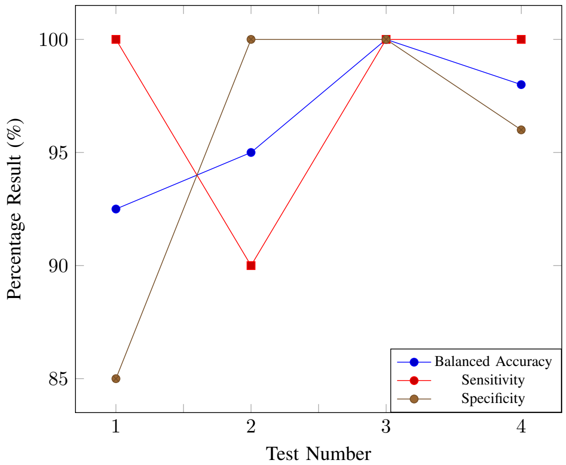

Fig. 6. Classification results for overall balanced accuracy, sensitivity and specificity for the highest performing classifier of a Bagged Tree Classifier

TABLE I
COMPARISON OF OVERALL CLASSIFICATION RESULTS BETWEEN SYSTEMS USING THE BAGGED TREE CLASSIFIER

Measures	**This System**	**RT-Fall [1]**	**WiFall [7]**
Balanced Accuracy	96 %	91 %	81 %
Sensitivity	98 %	91 %	79 %
Specificity	94 %	92 %	83 %
F1-Score	0.95	0.88	0.74

accuracy was used to compare to existing systems as it is not known if the test sets will be balanced. It was important to keep sensitivity and specificity high to detect all falls and minimise false alarms, respectively.

The system achieves a total of 96 % balanced accuracy, 98 % sensitivity, 94 % specificity and a F1-Score of 0.95 as shown in Table I. The variation in classification performance is shown in Fig. 6. The system is clearly very good at generalising for all activities given high statistics in all 4 areas. The specificity is high in all cases meaning there are few false alarms deeming our system quite appropriate for its purpose. The system was also tested in 2 other residential environments (LOS & NLOS through walls), namely kitchens and bedrooms, with 3 individuals present and a pet. The same number of falls were performed as Section IV-A and a balanced accuracy of 90 % and a F1-Score of 0.89 was achieved. The system outperforms both state-of-the-art solutions, RT-Fall [1] and WiFall [7] (tested by RT-Fall), as shown in Table I. Throughout 4 tests, the system obtains slightly higher sensitivity and specificity than RT-Fall. However, RT-Fall had access to a much larger training and test data-set which will hopefully be achieved as part of future work in this area.

V. CONCLUSION

In this paper, a wireless fall detection system using Channel State Information (CSI) of a Wi-Fi channel has been proposed. The system is cheap, accurate, non-intrusive and does not require the user to wear any devices. The CSI phase difference over 2 antennas is utilised for fall detection and a new type of fall, sitting falls, is proposed which was not explored by the current state-of-the-art systems, RT-Fall [1] & WiFall [7]. With the growth of smart home technologies, homes will eventually contain many Wi-Fi enabled sensors/devices, allowing for research of the application of this system across the home from one base AP.

VI. ACKNOWLEDGEMENTS

We would like to thank Mr. James Kinsella of Maynooth University for allowing access to the Radiospace - National 5G Test Centre to verify initial CSI pre-processing methods.

REFERENCES

[1] H. Wang, D. Zhang, Y. Wang, J. Ma, Y. Wang, and S. Li, "RT-Fall: A Real-Time and Contactless Fall Detection System with Commodity WiFi Devices," *IEEE Transactions on Mobile Computing*, vol. 16, pp. 511–526, Feb 2017.

[2] D. Wild, U. S. Nayak, and B. Isaacs, "How dangerous are falls in old people at home?," *British medical journal (Clinical research ed.)*, Jan 1981.

[3] J. M. Stokes, "Falls in older people: Risk factors and strategies for prevention (2nd edn) - by stephen lord, catherine sherrington, hylton menz, and jacqueline close," *Australasian Journal on Ageing*, vol. 28, no. 1, pp. 47–47, 2009.

[4] C. S. Florence, G. Bergen, A. Atherly, E. Burns, J. Stevens, and C. Drake, "Medical costs of fatal and nonfatal falls in older adults," *Journal of the American Geriatrics Society*, vol. 66, no. 4, pp. 693–698, 2018.

[5] S. M. Friedman, B. Munoz, S. K. West, G. S. Rubin, and L. P. Fried, "Falls and fear of falling: which comes first? A longitudinal prediction model suggests strategies for primary and secondary prevention," *Journal of the American Geriatrics Society*, Aug 2002.

[6] D. Halperin, W. Hu, A. Sheth, and D. Wetherall, "Tool Release: Gathering 802.11n Traces with Channel State Information," *ACM SIGCOMM CCR*, vol. 41, p. 53, Jan. 2011.

[7] Y. Wang, K. Wu, and L. M. Ni, "WiFall: Device-Free Fall Detection by Wireless Networks," *IEEE Transactions on Mobile Computing*, vol. 16, pp. 581–594, Feb 2017.

[8] K. Wu, J. Xiao, Y. Yi, M. Gao, and L. Ni, "FILA: Fine-grained indoor localization," *Proceedings - IEEE INFOCOM*, pp. 2210–2218, 03 2012.

[9] Y. Zhuo, H. Zhu, H. Xue, and S. Chang, "Perceiving accurate CSI phases with commodity WiFi devices," in *IEEE INFOCOM 2017 - IEEE Conference on Computer Communications*, pp. 1–9, May 2017.

[10] C. Wu, Z. Yang, Z. Zhou, K. Qian, Y. Liu, and M. Liu, "PhaseU: Real-time LOS identification with WiFi," in *2015 IEEE Conference on Computer Communications (INFOCOM)*, pp. 2038–2046, April 2015.

[11] A. Chadha, N. Satam, and B. Ballal, "Orthogonal Frequency Division Multiplexing and its Applications," *International Journal of Science and Research*, vol. 2, p. 325, 01 2013.

[12] S. Sen, B. Radunovic, R. R. Choudhury, and T. Minka, "You are facing the Mona Lisa: spot localization using PHY layer information," in *MobiSys '12*, 2012.

[13] IEEE802, "IEEE Standard for Information technology– Local and metropolitan area networks– Specific requirements– Part 11: Wireless LAN Medium Access Control (MAC)and Physical Layer (PHY) Specifications Amendment 5: Enhancements for Higher Throughput," *IEEE Std 802.11n-2009 (Amendment to IEEE Std 802.11-2007 as amended by IEEE Std 802.11k-2008, IEEE Std 802.11r-2008, IEEE Std 802.11y-2008, and IEEE Std 802.11w-2009)*, pp. 1–565, Oct 2009.